

Supplemental Materials and Methods

Bile acid quantification, continued. Total bile acids were quantified using a Mouse Total Bile Acid kit from Crystal Chem (Crystal Chem, Downers Grove, IL). To estimate the total bile acid pool, total liver bile acids, total gallbladder bile acids, and total bile acids from the small and large intestinal contents were measured and calculated per g of body weight. Small and large intestinal contents were homogenized and dried in a vacuum centrifuge at 37°C until the weight was stable (approximately 72 hours). The dried pulverized intestinal content, 50-100 mg homogenized liver or total gallbladder was extracted in 1.0 ml 75% ethanol at 50°C for 2 hours. All extracts were centrifuged at 4°C at 6000 g for 10 min, and 20 µl supernatant was used for bile acid detection according to the manufacturer's protocol.

To determine gallbladder weight, animals were fasted for 6 hours and the cystic duct was tied so that no bile could escape. The gallbladder was carefully removed and weighed. Most of the weight is contributed by bile. Therefore gallbladder weight provides a fair estimate of gallbladder content (1). Homogenized total gallbladder was used to quantify bile acid concentration in the gallbladder.

Biochemical analysis. Plasma alanine aminotransferase (ALT) level was quantified by Infinity ALT kit (Thermo Scientific, Middletown, VA). Plasma ethanol concentration was determined using the Ethanol Assay Kit (BioVision, Milpitas, CA). Hepatic triglyceride concentrations were quantified using the Triglyceride Liquid Reagents Kit (Pointe Scientific, Canton, MI) as previously described (2). Bilirubin plasma concentration was measured by colorimetric detection using QuanticChrom Bilirubin Assay Kit (DIBR-180, BioAssay System, Hayward, CA) following the manufacturer's protocol.

Staining procedures. Formalin-fixed and paraffin-embedded livers were stained with hematoxylin-eosin (Surgipath, Buffalo Grove, IL) using standard staining protocols. For

hepatic lipid accumulation analysis, frozen sections were cut and stained with Oil Red O.

Real-time quantitative polymerase chain reaction (qPCR). RNA was extracted from mouse tissue using Trizol (Invitrogen, Carlsbad, CA). RNA was digested with DNase using the DNA-free DNA removal kit (Ambion, Carlsbad, CA) and reverse transcribed using the High Capacity cDNA Reverse Transcription kit (Applied Biosystems, Foster City, CA). Gene expression was detected with Universal SYBR Green Supermix (Bio-Rad, Hercules, CA) as described (3, 4) using gene specific primer sets with 18S as housekeeping gene (sequences were all from NIH qPrimerDepot). To quantify intestinal bacteria, DNA was extracted from adherent and luminal intestinal contents as described (2). DNA was amplified using published 16S rRNA primer sets for universal bacteria (5) and SYBR Green. To determine the total bacterial load present in the cecum, the qPCR value for each sample was multiplied by the total amount of DNA per gram of cecal content.

Immunoblot analyses and ELISA. Liver microsomes and liver whole cell lysates were extracted for immunoblot as described (2). Immunoblot analysis was performed as described (2) using anti-Cyp7a1 (Abcam, Cambridge, MA), anti-Cyp8b1 (Santa Cruz Biotechnology, Dallas, TX), anti-Cyp27a1 (Santa Cruz Biotechnology, Dallas, TX), anti-Shp (Santa Cruz Biotechnology, Dallas, TX), anti-Cyp2e1 (Millipore Corporation, Billerica, MA), anti-Akt (Santa Cruz Biotechnology, Dallas, TX), anti-p-Akt (Cell Signaling, Beverly, MA), anti-Erk1/2 (Cell Signaling, Beverly, MA), anti-p-Erk1/2 (Santa Cruz Biotechnology, Dallas, TX), and anti-occludin (Invitrogen, Camarillo, CA). Anti-tubulin (Santa Cruz Biotechnology, Dallas, TX), anti-VDAC1 (Abcam, Cambridge, MA), anti- β -actin (Sigma-Aldrich, St. Louis, MO) antibodies were used as loading control. Densitometry of immunoblot analysis was performed using NIH ImageJ. Fecal albumin was determined by ELISA (Bethyl Labs, Montgomery, TX) as described (2). Whole liver

cell lysates for ELISA were extracted using a buffer containing 100 mM Tris (pH 7.4), 150 mM NaCl and protease inhibitors (Roche, Indianapolis, IN). ELISA was used to quantify hepatic interleukin (IL)-1B and tumor necrosis factor (TNF) (eBioscience, San Diego, CA), and FGF15 (Uscn Life Science Inc., Houston, TX). Plasma FGF15 results were confirmed with High Sensitive FGF15 ELISA kit from Mybiosource (#MBS2087082, San Diego, CA). Plasma M52 levels were quantified using FGF19 ELISA kit purchased from Biovendor (Asheville, NC).

Supplemental Figure Legends

Supplemental Figure 1. Gallbladder weight increases after alcohol feeding.

C57BL/6 mice were fed an oral control diet (n=5–9) or ethanol diet (n=8) for 8 weeks. (A) Gallbladder weight at time of harvesting. (B) Bile acid composition ratio in gallbladder. (C) Bile acid concentrations in urine. *P < 0.05. Abbreviations: BA, bile acid; CA, cholic acid; DCA, deoxycholic acid; EtOH, ethanol; HDCA, hyodeoxycholic acid; MCA, muricholic acid; T-CA, taurocholic acid; T-DCA, taurodeoxycholic acid; T-MCA, taumuricholic acid.

Supplemental Figure 2. Alcohol decreases ileal FGF15 protein concentrations.

C57BL/6 mice were fed an oral control diet (n=6) or ethanol diet (n=12) for 8 weeks. FGF15 concentration measured from ileum tissue by ELISA. *P < 0.05. Abbreviations: EtOH, ethanol; FGF15, fibroblast growth factor 15.

Supplemental Figure 3. Impact of alcohol on bile acid-related pathways.

C57BL/6 mice were fed an oral control diet (n=5) or ethanol diet (n=8–12) for 8 weeks. (A) Immunoblot of hepatic Cyp8b1 and Cyp27a1. (B) Immunoblot of hepatic phospho-Erk1/2, Erk1/2, phospho-Akt, Akt. (C) Bilirubin plasma level. Abbreviations: Akt, Protein kinase B;

Cyp8b1, sterol 12 α -hydroxylase; Cyp27a1, Sterol 27-hydroxylase; Erk, Extracellular signal-regulated kinase.

Supplemental Figure 4. Alcohol does not cause significant changes in expression of bile acid transporters in liver and gut. C57BL/6 mice were fed an oral control diet (n=4-10) or ethanol diet (n=8–12) for 8 weeks. (A) Expression of *Ntcp*, *Bsep*, *Mrp3*, *Mrp4* mRNA in liver. (B) Expression of *FXR*, *Shp*, *Asbt*, *Ost-a*, *Ost-b*, *Fabp6* mRNA in ileum. Abbreviations: *Asbt*, Apical sodium-dependent bile acid transporter; *Bsep*, Bile salt export pump; EtOH, ethanol; *Fabp6*, Fatty acid binding protein 6; *FXR*, Farnesoid X receptor; *Mrp3/4*, Multidrug resistance-associated protein 3/4; *Ntcp*, Na(+)/taurocholate transport protein; *Shp*, Small heterodimer partner; *Ost-a/-b*, Organic solute transporter alpha/beta.

Supplemental Figure 5. Hepatic *Srebp1* and *Cidea* gene expression is not affected by antibiotics. C57BL/6 mice were fed an oral control diet or ethanol diet for 8 weeks (n=9). Antibiotics polymyxin B and neomycin were administered during the last 4 weeks of feeding. Expression of *Srebp1*, *Cidea* mRNA in liver. Abbreviations: Abx, antibiotics; *Cidea*, Cell death-inducing DNA fragmentation factor α -like effector A; EtOH, ethanol; *Srebp1*, sterol response element-binding 1.

Supplemental Figure 6. Absorption and hepatic metabolism of ethanol after fexaramine. C57BL/6 mice were fed an oral control diet (n=6) or ethanol diet (n=7–12), and also given vehicle (corn oil) or fexaramine for 8 weeks. (A) Plasma level of ethanol at time of harvesting. (B) Hepatic expression of *Adh1* mRNA. (C) Immunoblot analysis of hepatic *Cyp2e1*. Abbreviations: *Adh1*, alcohol-dehydrogenase 1; *Cyp2e1*, cytochrome P450 family 2 subfamily E member 1; EtOH, ethanol.

Supplemental Figure 7. Fexaramine leads to intestinal FXR activation, reduction of intestinal inflammation, and protects from alcohol-induced gut barrier dysfunction.

C57BL/6 mice were fed an oral control diet (n=5–10) or ethanol diet (n=12–17), and also given vehicle (corn oil) or fexaramine for 8 weeks. (A) Total cecal bacteria were assessed by qPCR. (B) Fecal albumin concentrations. (C) Immunoblot analysis of Ocln (occludin) in the small intestine. (D) Expression of *Tnf* and *Il1b* mRNA in intestine. (E) Immunoblot analysis of intestinal Shp. **P* < 0.05. Abbreviations: EtOH, ethanol; *Il1b*, interleukin-1 beta; Ocln, Occludin; Shp, Small heterodimer partner; *Tnf*, tumor necrosis factor.

Supplemental Figure 8. Hepatic Srebp1 and Cidea gene expression is not affected by fexaramine.

C57BL/6 mice were fed an oral control diet (n=5) or ethanol diet (n=12–14), and also given vehicle (corn oil) or fexaramine for 8 weeks. Expression of *Srebp1*, *Cidea* mRNA in liver. Abbreviations: *Cidea*, Cell death-inducing DNA fragmentation factor α -like effector A; EtOH, ethanol; *Srebp1*, Sterol response element-binding 1.

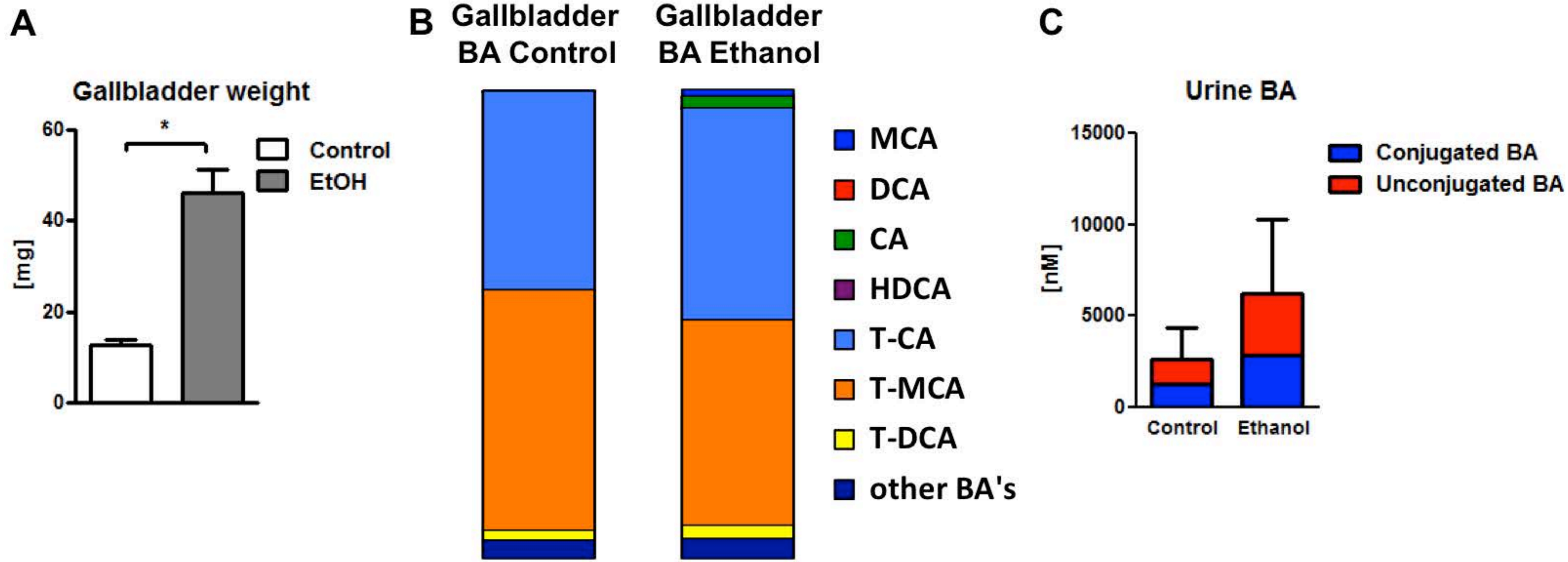
Supplemental Figure 9. Absorption and hepatic metabolism of ethanol after AAV-M52 injection.

C57BL/6 mice were fed an oral control diet (n=6) or ethanol diet (n=5–15). Mice were injected adeno-associated virus with FGF19-variant M52 (AAV-M52) or AAV-GFP as control 3 weeks after liquid diet feeding was started. (A) Plasma level of ethanol at time of harvesting. (B) Hepatic expression of *Adh1* mRNA. (C) Immunoblot analysis of hepatic *Cyp2e1*. (D) Plasma concentrations of M52. (E) Expression of *Srebp1*, *Cidea* mRNA in liver. **P* < 0.05. Abbreviations: AAV, adeno-associated virus; *Cidea*, Cell death-inducing DNA fragmentation factor α -like effector A; EtOH, ethanol; GFP, green fluorescent protein; M52, fibroblast growth factor 19-variant M52; *Srebp1*, Sterol response element-binding 1.

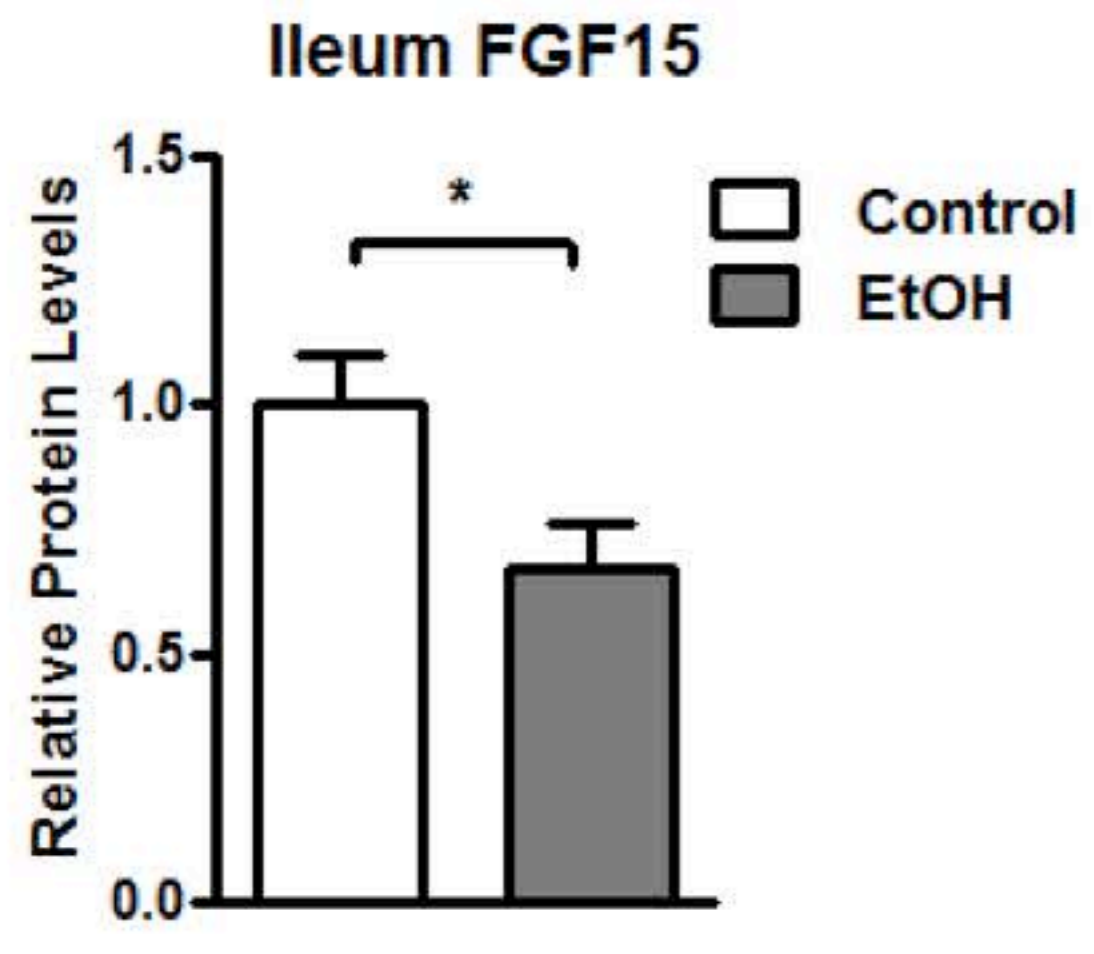
References

1. Khanuja B, Cheah YC, Hunt M, Nishina PM, Wang DQ, Chen HW, et al. Lith1, a major gene affecting cholesterol gallstone formation among inbred strains of mice. *Proc Natl Acad Sci U S A*. 1995;92(17):7729-33. PubMed PMID: 7644485; PubMed Central PMCID: PMC41219.
2. Hartmann P, Chen P, Wang HJ, Wang L, McCole DF, Brandl K, et al. Deficiency of intestinal mucin-2 ameliorates experimental alcoholic liver disease in mice. *Hepatology*. 2013;58(1):108-19. Epub 2013/02/15. doi: 10.1002/hep.26321. PubMed PMID: 23408358; PubMed Central PMCID: PMC3695050.
3. Tacke F, Gabele E, Bataille F, Schwabe RF, Hellerbrand C, Klebl F, et al. Bone morphogenetic protein 7 is elevated in patients with chronic liver disease and exerts fibrogenic effects on human hepatic stellate cells. *Dig Dis Sci*. 2007;52(12):3404-15. Epub 2007/04/07. doi: 10.1007/s10620-007-9758-8. PubMed PMID: 17415633.
4. Wang L, Hartmann P, Haimerl M, Bathena SP, Sjowall C, Almer S, et al. Nod2 deficiency protects mice from cholestatic liver disease by increasing renal excretion of bile acids. *J Hepatol*. 2014;60(6):1259-67. Epub 2014/02/25. doi: 10.1016/j.jhep.2014.02.012. PubMed PMID: 24560660; PubMed Central PMCID: PMC4028388.
5. Horz HP, Vianna ME, Gomes BP, Conrads G. Evaluation of universal probes and primer sets for assessing total bacterial load in clinical samples: general implications and practical use in endodontic antimicrobial therapy. *J Clin Microbiol*. 2005;43(10):5332-7. Epub 2005/10/07. doi: 10.1128/JCM.43.10.5332-5337.2005. PubMed PMID: 16208011; PubMed Central PMCID: PMC1248440.

Supplemental Figure 1

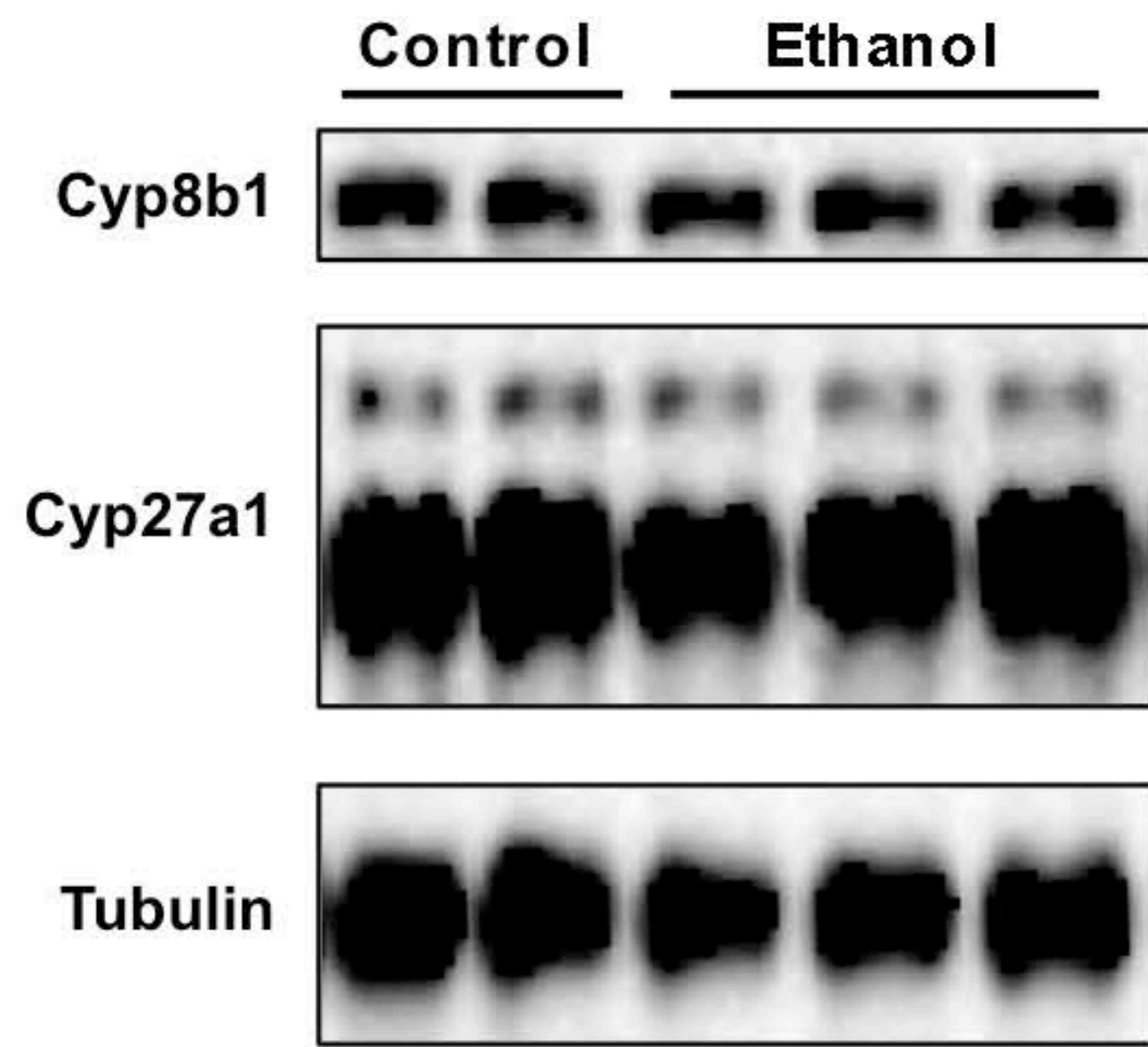


Supplemental Figure 2

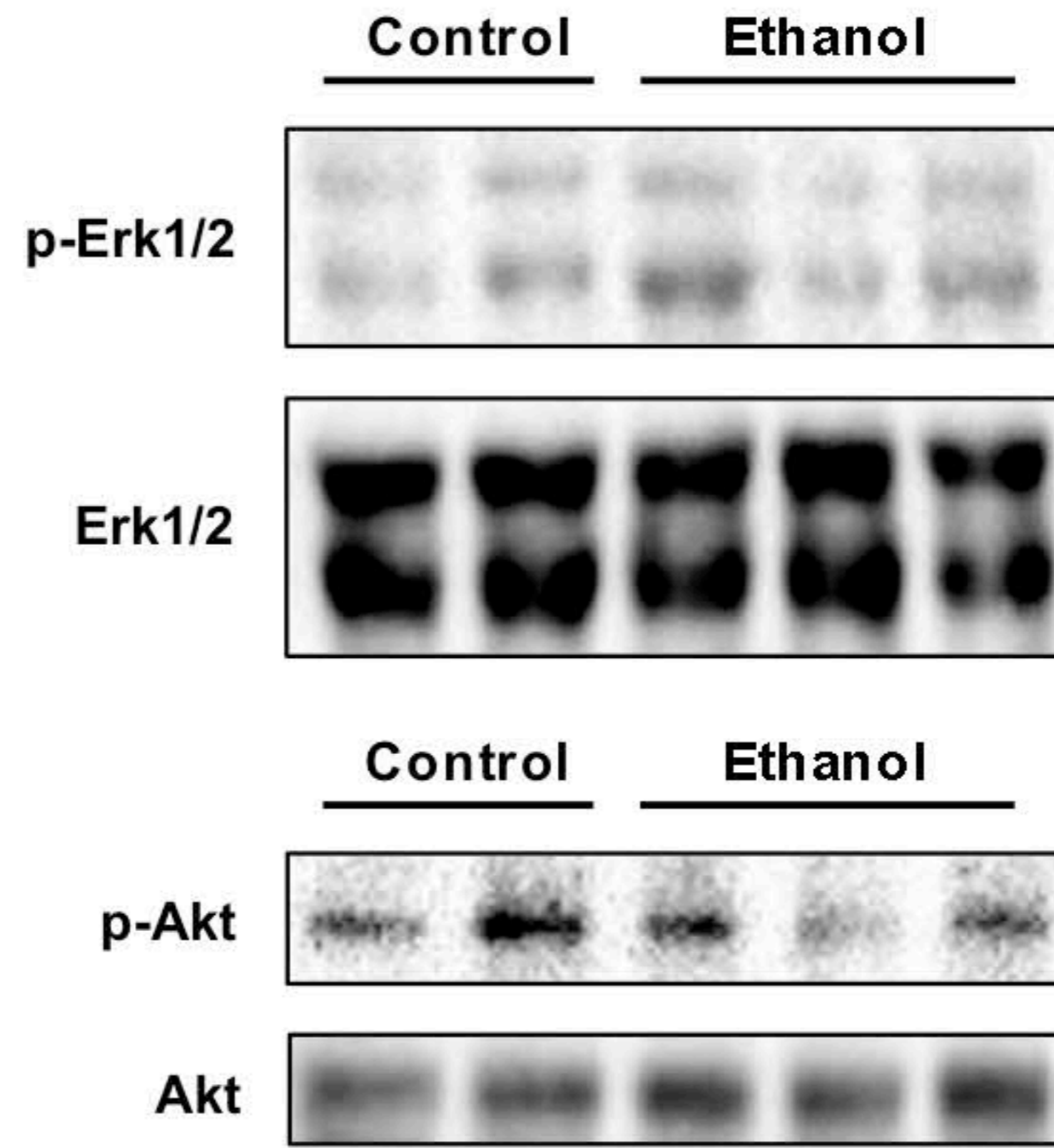


Supplemental Figure 3

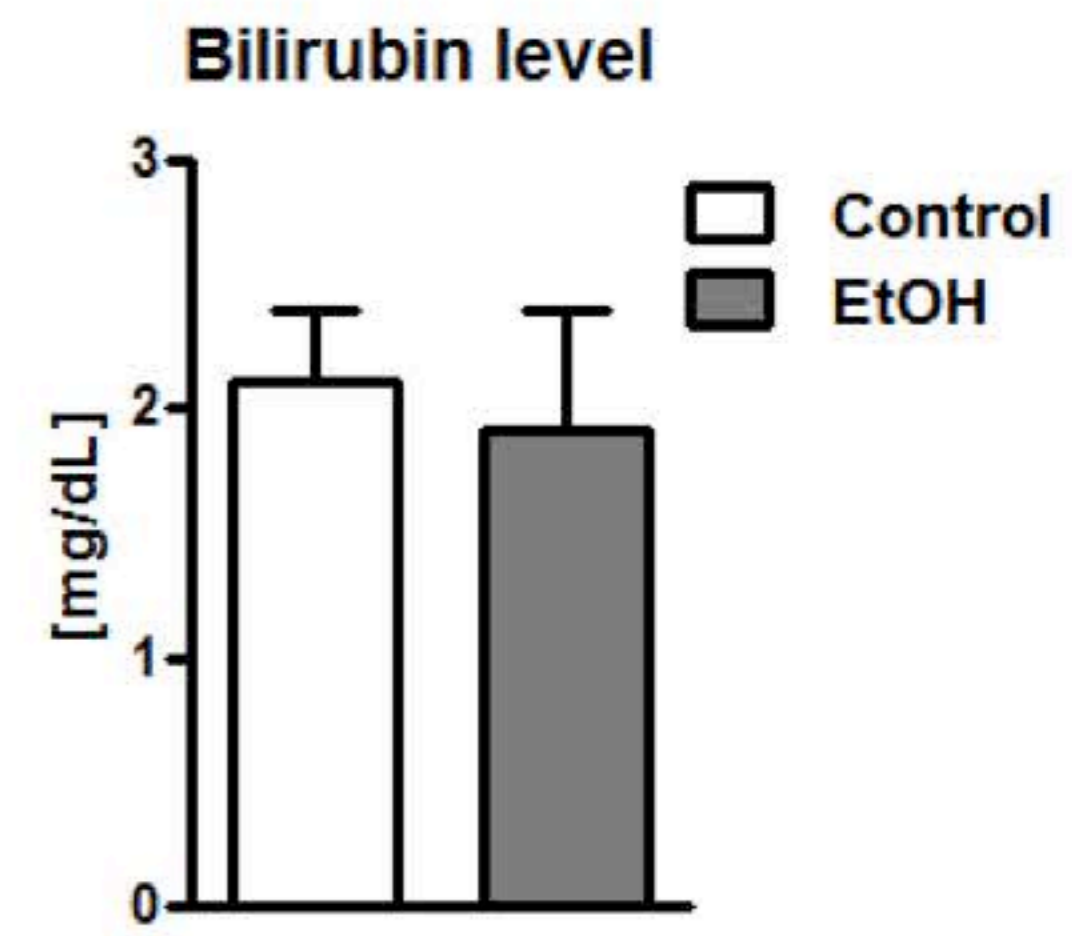
A



B

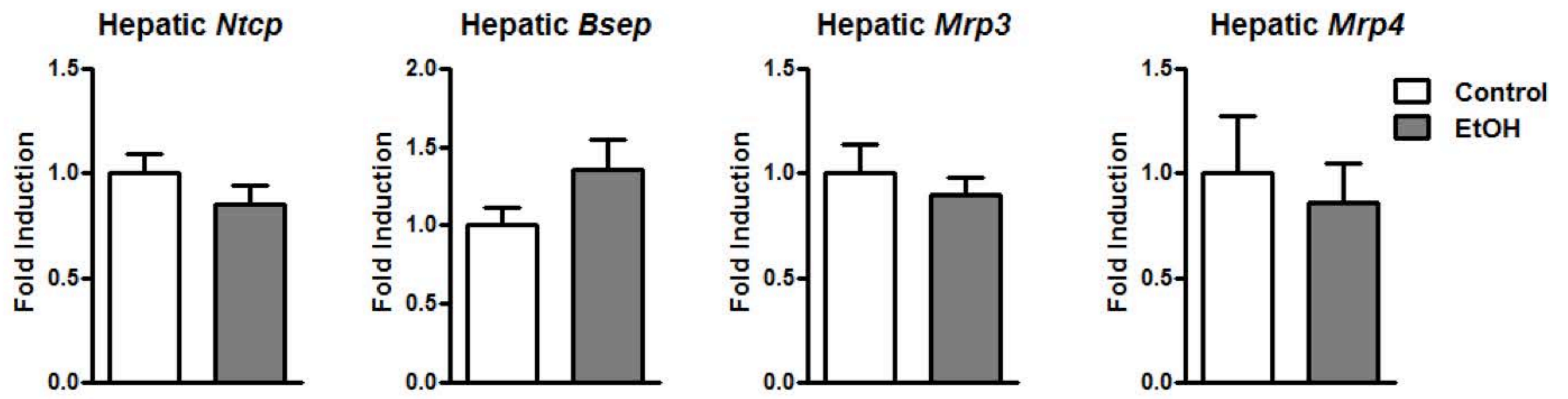


C

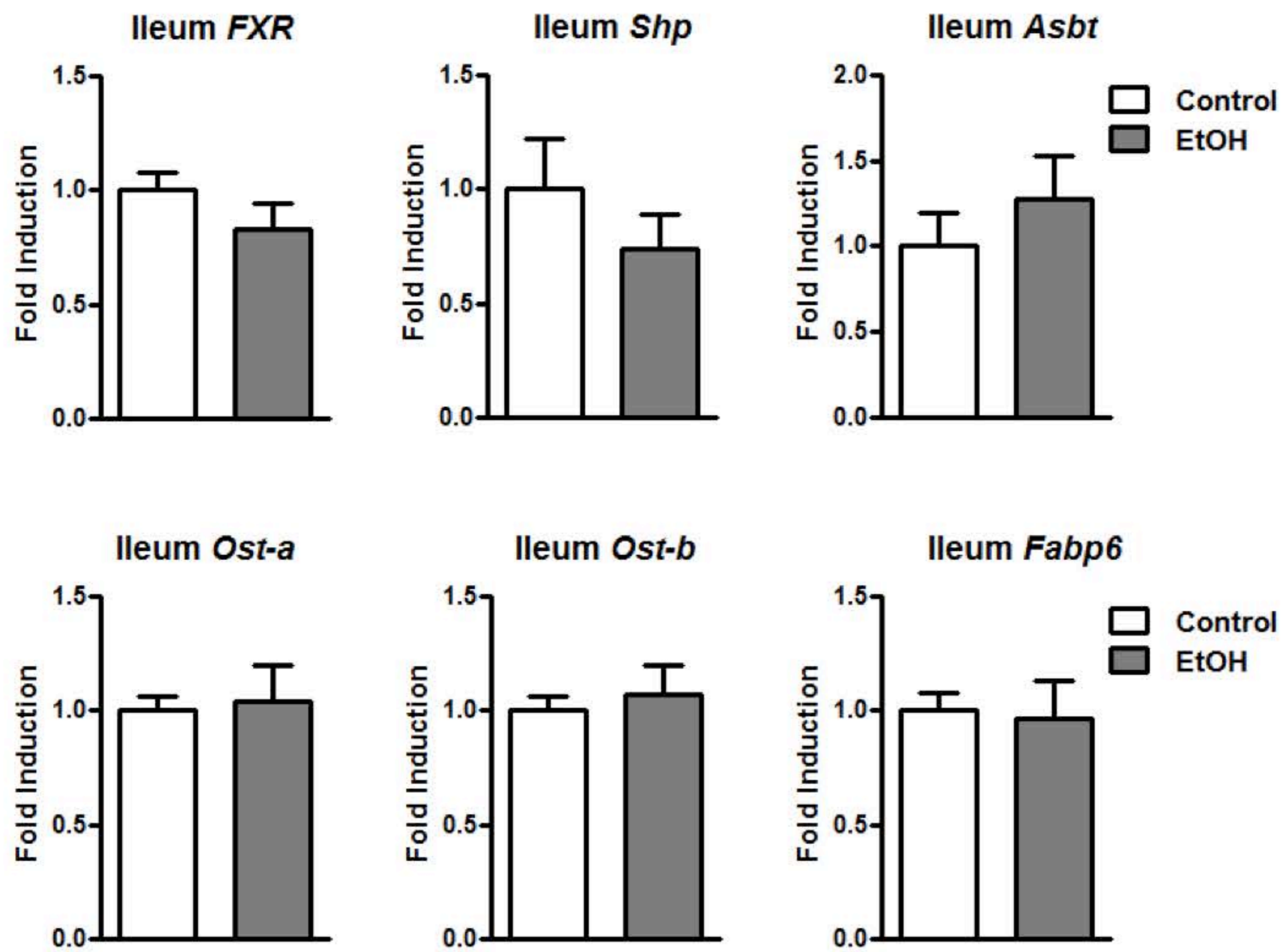


Supplemental Figure 4

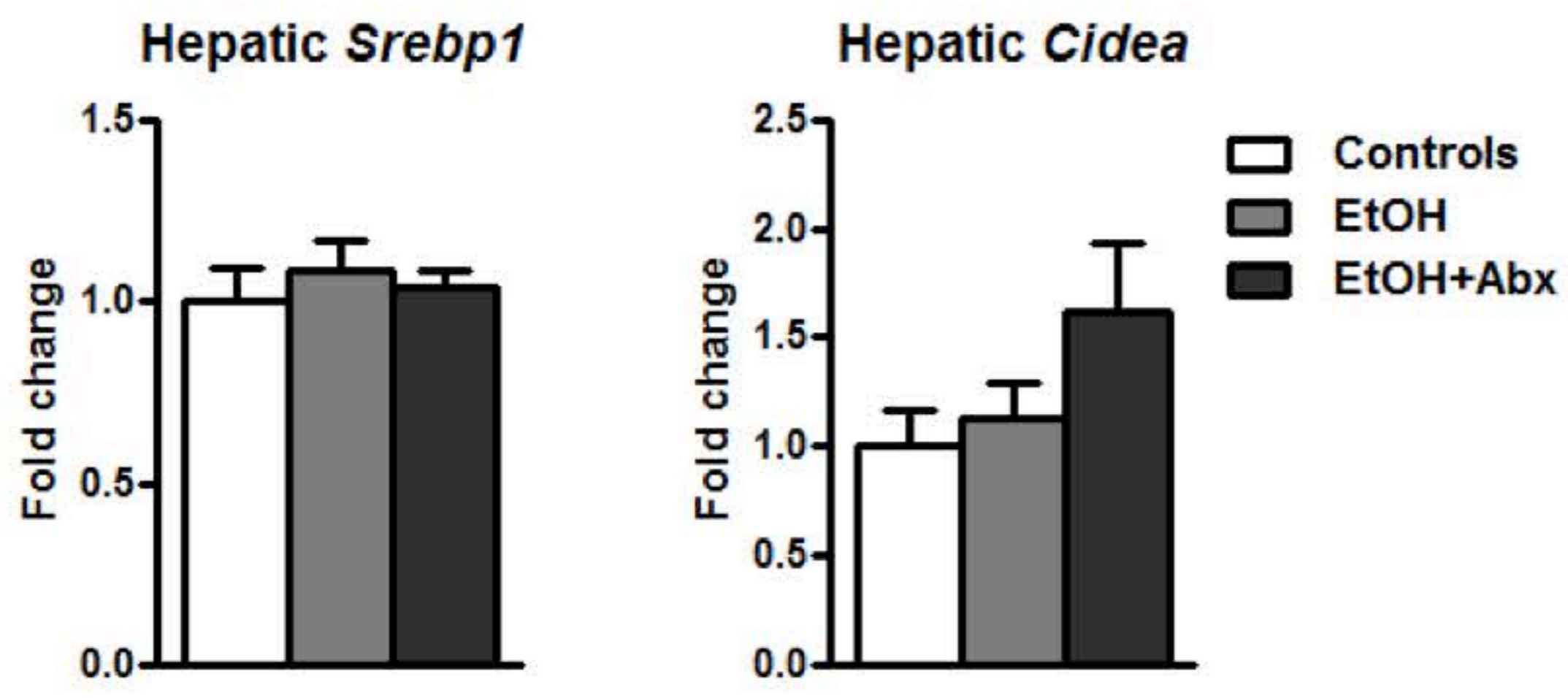
A



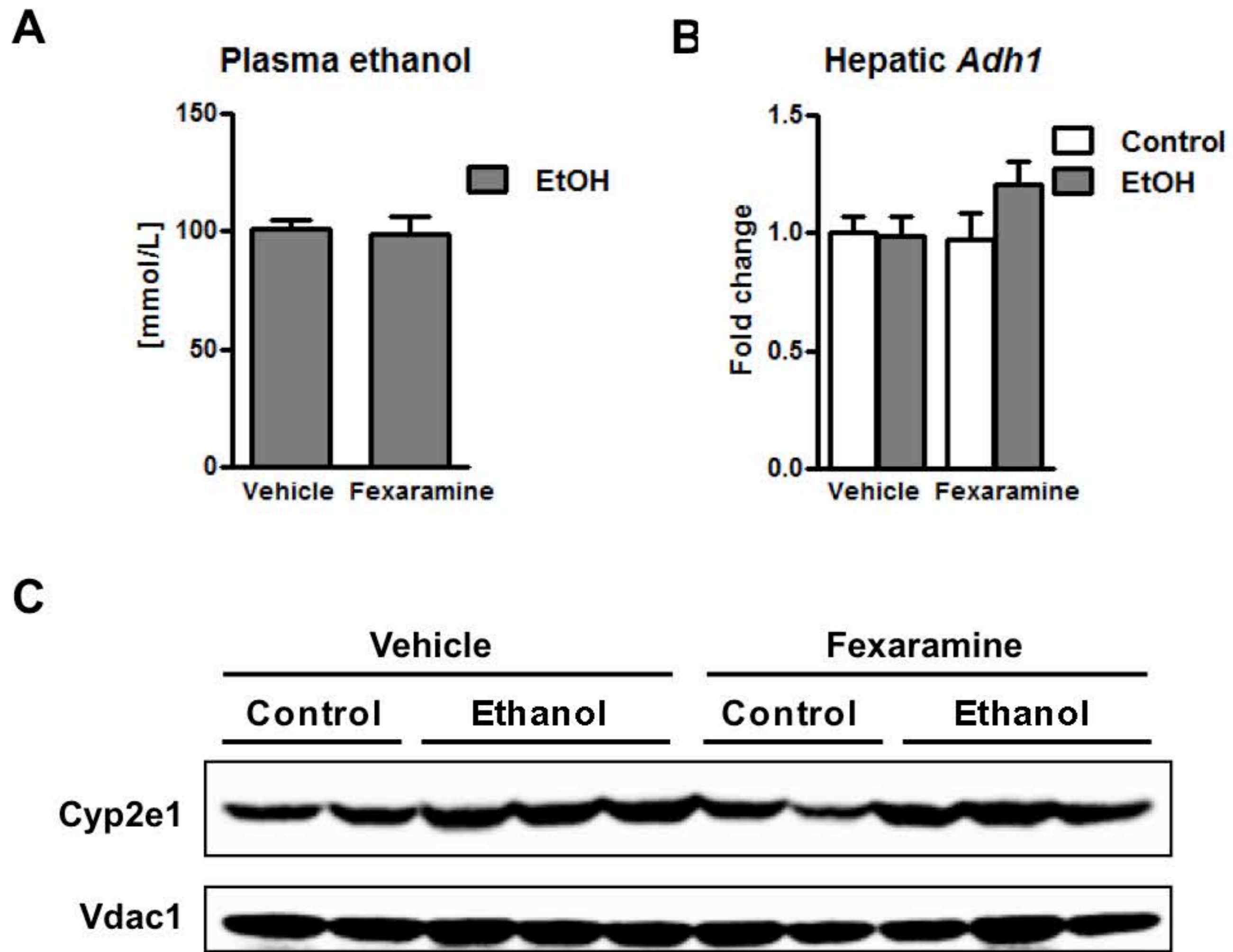
B



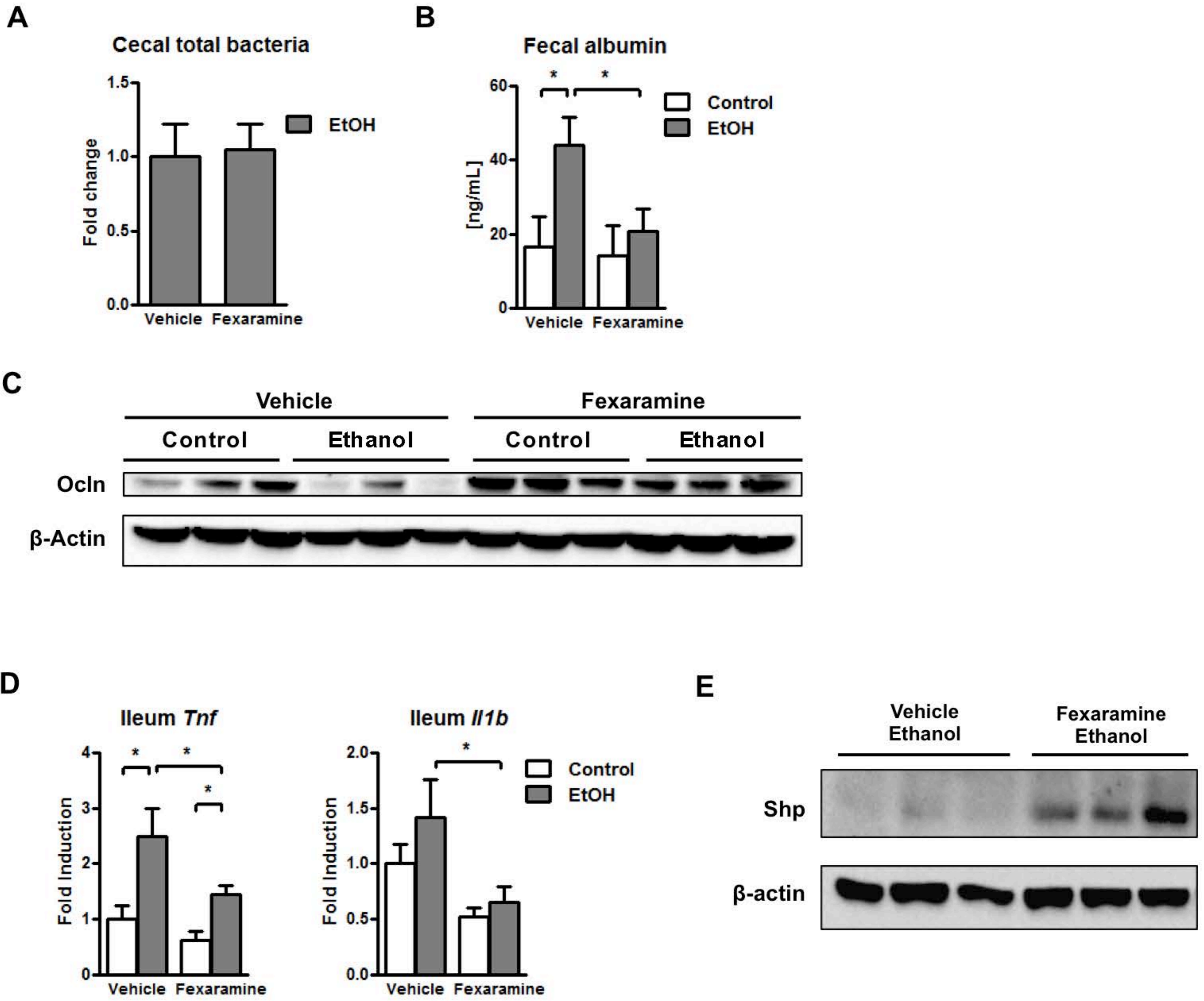
Supplemental Figure 5



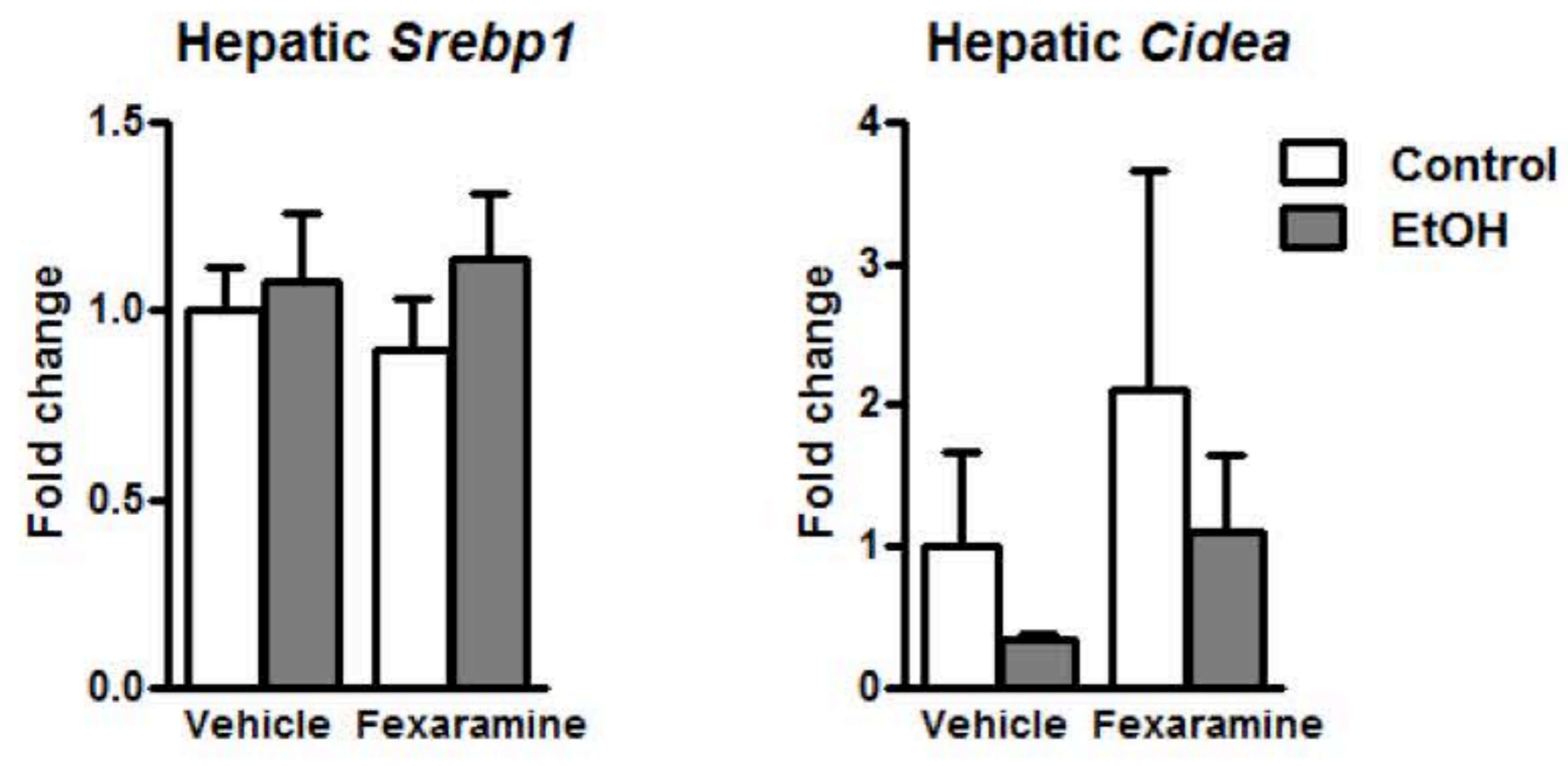
Supplemental Figure 6



Supplemental Figure 7



Supplemental Figure 8



Supplemental Figure 9

